Linear augmented Slater-type-orbital study of Au—5d-transition-metal alloying

R. E. Watson, J. W. Davenport, and M. Weinert
Physics Department, Brookhaven National Laboratory, Upton, New York 11973-5000
(Received 11 September 1986)

We have used density-functional theory with an augmented Slater-type-orbital basis to calculate the heat of formation and crystal structure for the 5d-transition-metal—gold alloys AuLu through AuPt. The crystal structures considered were CsCl, CuAuI, γ-CuTi, $MoSi_2$, Au_2Nb_3, Cu_3Au, Cr_3Si, and AlB_2, though not all structures were calculated for each compound. There are no experimental values for the heats but our results are consistent with known phase diagrams. In several instances we find suppression of a phase at 50%-50% by another off 50%-50%. We have also calculated the charge transfer using Mulliken and Wigner-Seitz sphere counts. These do not follow electronegativity trends but are consistent with calculated initial-state core-level shifts and Mössbauer isomer shifts (obtained from the calculated contact density).

I. INTRODUCTION

The noble metals, lying between the transition and the main-group elements in the Periodic Table, have had a special place in our understanding of alloying. Over fifty years ago Hume-Rothery noted[1] that the phase boundaries, due to alloying with simple metals, tended to occur at well-defined electron-to-atom ratios. As originally formulated, this view neglects any participation by the filled noble-metal d bands in the bonding. The noble metals also display[2–4] transition-metal characteristics when alloyed, and this is because the d bands are active chemically due to hybridization with the electron orbitals of the other alloy constituents. A noble metal in an alloy may appear to be gaining valence-electron charge according to one experimental probe while losing it according to another and, for Au, this was explained[2] in terms of counter d and non-d charge flow. Among the noble metals, Au is of particular interest since by a number of measures it is the most electronegative of the metallic elements, i.e., the strongest competitor for the other alloy constituent's valence-electron charge. Electronic structure calculations, which explore the energetics and the charge transfer in Au alloyed with the 5d-transition-metal elements in different phases at several different alloy compositions, are reported in this paper.

The present investigations employ the linearized-Slater-type-orbital method[5,6] (LASTO), with the local-density approximation. The calculations are scalar relativistic, that is, spin-orbit coupling has been omitted from the conduction bands. The core levels are treated fully relativistically. In addition, muffin-tin potentials, which involve spherical potentials within the atomic spheres, have been used. One purpose of the present paper is to test the applicability of this class of potential to the calculation of the energy of one phase relative to others. It will be seen that the approximation works well provided that the phases being compared are close packed, that is fcc-, hcp-, or bcc-like. This is the case for a number of the competing phases appropriate to the Au alloys and their calculated heats of formation (which involve differences between their total energies and the total energies of the elemental metals which are also close packed) appear to be accurate. Not surprisingly, the muffin-tin approximation does not work well in placing the energy of an ill-packed structure, which has sites of intrinsically low geometric symmetry, with respect to those of the close-packed systems. An example of this will be seen.

The crystal structures of concern are inspected in Sec. II. This is followed by consideration of the calculated heats of formation, ΔH. There are no experimental data for the Au systems dealt with here, but the trends in the ΔH are consistent with known phase-diagram behavior and the stable phases are correctly predicted for the 50%-50% alloys. Calculations for the close-packed phases at different compositions correctly display cases where a phase at one composition suppresses a phase at another and other cases where the two phases both exist, i.e., features of the $T=0$ phase diagrams are being correctly reproduced.

Four measures of charge transfer are then considered. Two are related to experimental observables: the electron density at the nucleus and the potential-energy contributions to the core-electron one-electron energy shifts due to alloying. The third measure involves integrating the valence-electron charge within Wigner-Seitz spheres, while the last exploits the Slater-type-orbital character of the wave functions outside the muffin-tin spheres to make orbital population analyses of the valence charge *centered* on a site, though extending into neighboring sites. These various measures display the counterflow of d versus non-d charge at the Au sites, which was discussed above, with the net charge flow onto Au. Such d compensation is often not observed for the other constituent. The Wigner-Seitz (WS) sphere charges and the orbital populations mimic each other but are not in sufficient numerical agreement to make detailed common statements concerning charge transfer. There is one important feature they share: On going from Pt alloyed with Au across the 5d row to Hf and Lu one would expect, based on electronegativity arguments, that the charge transfer onto Au increases. This is not the case. It increases on going from

Au-Pt to Au-W, levels on going to Au-Ta, and drops on going to Au-Hf and, in turn, Au-Lu. Lu and Hf may lose valence charge more readily than do the other $5d$ elements when involved in ionic bonding but apparently interband hybridization arrests this trend when these elements are alloyed with Au.

There is another important feature of the charge transfer observed in the present results which apparently has not been discussed previously in the literature. High-l components are carried in the charge density at an atomic site, and these may be viewed as associated with the tails of s-, p, and d-like band orbitals centered on neighboring sites. This tail charge is substantial, as measured by the $l \geq 3$ charge components in the WS spheres of the elemental metals and, because the amount of this tailing varies from element to element, there is a significant change in the tail charge at a site upon alloying. This overlap charge, which has nothing to with orbital hybridization or screening in the normal sense, is a significant component of charge transfer in these Au alloys. Such overlap must join s, p, and d electron population changes in any numerical accounting of charge transfer.

II. THE CRYSTAL STRUCTURE

Inspection of the crystallographic[7] and phase diagram data for the ordered Au-$5d$ compounds shows several closely related crystal structures to occur, which involve a few atoms per unit cell. These are summarized in Fig. 1. First there is the cubic CsCl structure with one atomic species at the cube corners and another at the cube center. Like atoms are thus in (100) planes which are stacked *ABAB* etc. as is shown. The CuAuI structure (not shown) is obtained by a tetragonal distortion along the c axis normal to these planes so the c/a ratio goes from 1.0, characteristic of the CsCl structure, to $\leq\sqrt{2}$. The remaining γ-CuTi, $MoSi_2$, and Nb_3Au_2 structures involve different stackings of (100) planes in the bcc lattice. The Nb_3Au_2 structure, with its *AAABB* stacking, is one of the simplest compound structures with two species of majority atom sites. One of these has *all* like nearest neighbors (the A layers sandwiched between A's) while the other site is involved in nearest-neighbor bonding with unlike B atoms. As will be seen, the Ta valence charge character is very different at these two sites.

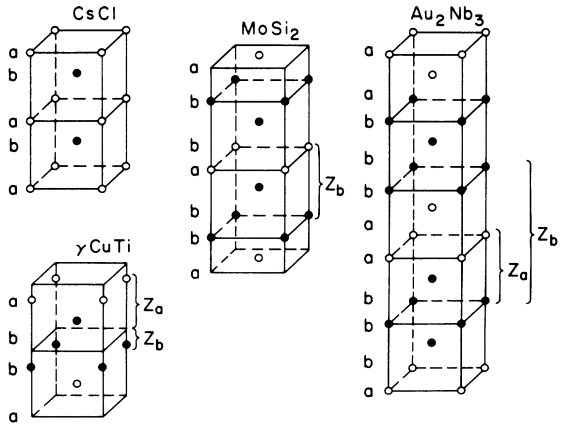

FIG. 1. Some of the crystal structures encountered as Au-$5d$ element phases. Single unit cells are shown, except for the CsCl structure where two cells are drawn.

All the above, except for the CsCl, are tetragonal systems. Thus their total energies depend on c/a ratios as well as on lattice volumes. Any distortion off of the correct c/a or volume corresponds to an acoustic phonon. More serious, the $MoSi_2$ involves one, and the γ-CuTi and Nb_3Au_2 two, internal coordinates which are not determined by symmetry and which place the positions of the atomic planes with respect to the c axis. Any error in these positions corresponds to excitations of optical phonons with their substantially larger energies. Moreover, these internal coordinates have been obtained experimentally for only one of the systems of concern here and there is some question of its accuracy. The variation in total energy with these coordinates can be substantial, on the scale important to the stability of one crystal structure relative to another, and ascertaining optimum coordinates significantly increases the magnitude of the band-theory investigations. The sensitivity of the total energies to such coordinates will be indicated in Sec. IV.

Three other crystal structures will be considered. First, there is the cubic Cu_3Au structure where one atomic species residues on the cube corners and the other on the centers of the cube faces of an fcc lattice: Au_3Pt orders in this structure. The remaining two structures are worse packed and involve lower site symmetries than do those above. Their inclusion offers a test of how well the muffin-tin potentials, used here, can yield the relative total energies of quite differently packed systems. One system is the cubic $A15$ or Cr_3Si structure with its close-lying linear chains of atoms along cube faces. Au-Ta forms in this structure though at 4:1 rather than the stoichiometric 3:1 concentration. The other structure is AlB_2 where the B's form graphitic planes with the Al's in hexagonal planes, of half the atomic density, between them. No Au-5d compound forms in this phase but Au_2Nb (and Cu_2La) have been reported. It will be of interest to inspect Au_2Ta in this structure in competition with other Au-Ta phases at other concentrations.

III. TOTAL ENERGIES OF THE 50%-50% COMPOUNDS

Calculations were done based on the observed atomic volumes for AuLu, AuHf, and AuPt. Lacking such data for the W, Re, Os, and Ir systems, the alloy volume was taken to be the concentration-weighted average of the elemental metal volumes, i.e.,

$$V(A_xB_{1-x}) = xV_A + (1-x)V_B \ , \tag{1}$$

and the observed molecular volume of Au_2Ta_3 was scaled to 50%-50% concentration for AuTa. The resulting heats of formation appear in Fig. 2.

Positive, that is nonbinding, heats are obtained for the W, Re, Os, and Ir systems consistent with the fact that these systems form no ordered compounds and have little or no substitutional alloy solubility. The CsCl structure is calculated to be the most stable for AuLu, and the γ-CuTi

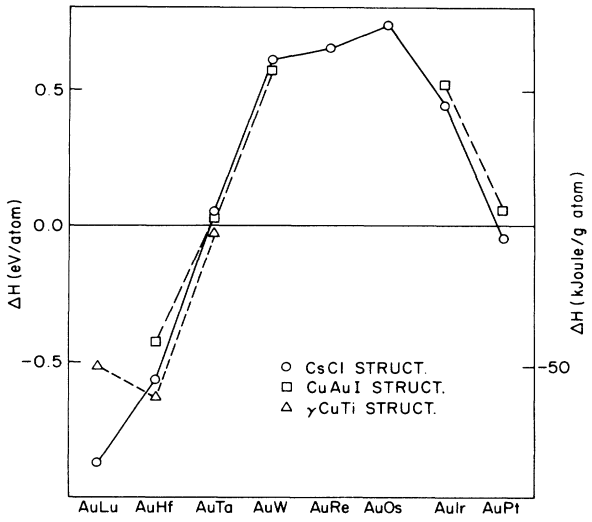

FIG. 2. Calculated heats of formation of 50%-50% Au-5d element phases.

most stable for AuHf. This agrees with experiment. The ordered AuTa and AuPt phases are not observed experimentally and are calculated to be weakly binding. This is consistent with their known phase-diagram behavior: Ordered AuPt loses out to a disordered fcc alloy while, as will be seen in the next section, the 50%-50% AuTa is suppressed by competition from a phase at another composition. To our knowledge, there are no experimental heats of formation for these alloy systems but the overall trend of negative, positive, and near-zero heats in Fig. 2 is consistent with the observed phase-diagram behavior. In addition, the correct ordered phases are predicted in the two cases where they are known.

Granted that Ta, Pt, and Au are fcc metals and PtAu a disordered fcc alloy, it is somewhat surprising, though not contrary to experiment, that of the ordered alloys, the CsCl structure prevails over the fcc-like CuAuI for AuIr and AuPt. This issue is explored further in Fig. 3; as noted earlier, the two structures are related to one another by a tetragonal distortion and the calculated heat of formation is plotted as a function of the associated c/a ratio. A c/a value of 1 corresponds to CsCl and that of $\sqrt{2}$ to "cubic" CuAuI, where the three lattice constants are equal. As a rule the CuAuI is distorted with a somewhat smaller c/a value and the minimum in the binding is obtained here.

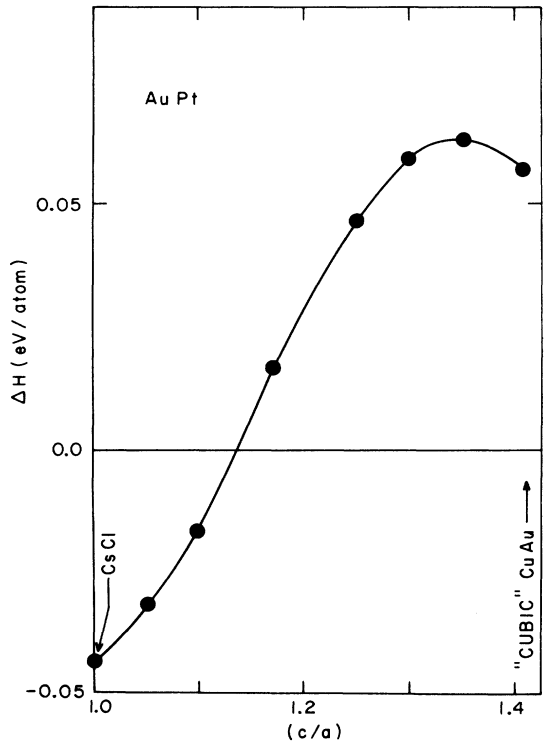

FIG. 3. Heat of formation of AuPt as a function of the c/a ratio associated with the tetragonal distortion connecting the CsCl and CuAuI structures. Systems ordering in the CuAuI structure are usually distorted with $1.30 < c/a < 1.35$.

IV. TOTAL ENERGIES FOR COMPOUNDS OFF 50%-50% CONCENTRATION

The $MoSi_2$ structure with its *abbabb* stacking occurs for $AuHf_2$ and Au_2Hf. Their calculated heats of formation are plotted in Fig. 4. The fact that the $AuHf_2$ heat lies below the line drawn between AuHf and Hf, implies that it is stable relative to a two-phase mix of AuHf and pure Hf at the same concentration, and similarly, Au_2Hf is predicted to be stable relative to AuHf and pure Au. Finally, the fact that the AuHf heat lies below the line between $AuHf_2$ and Au_2Hf implies that it is stable relative to a two-phase mixture of the latter. In making such constructs we are ignoring other competing phases at other compositions and are thus constructing a metastable phase diagram with such omissions. It should be noted[8] that the thermodynamic rules for constructing such metastable diagrams are the same as those for the full diagrams, and that is what has been done, for $T=0$, here.

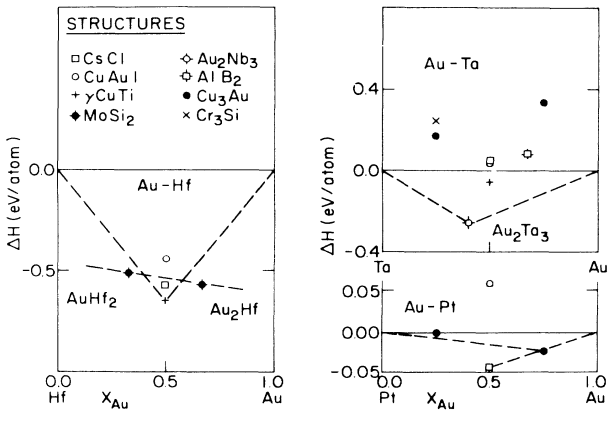

FIG. 4. Heats of formation for various phases of Au-Hf, Au-Ta, and Au-Pt as a function of alloy composition. Note the factor of 4 magnification of the Au-Pt energy scale.

[Most important of the omitted phases is Au_3Hf (Cu_3Ti structure) which has a relatively high melting temperature. With its eight atoms per unit cell, and several internal coordinates which require exploration, it proved too costly to investigate here.]

As was discussed in Sec. II the $MoSi_2$ structure involves one, and the CuTi structure in which AuHf forms involves two, internal coordinates which are not determined by the lattice constants and the crystal symmetry. Binding energies as a function of such coordinates appear in Fig. 5.

In these structures these coordinates provide the distances between stacking planes and for AuHf and $AuHf_2$ (and Au_2Ta_3) they have not been determined experimentally. $Z_a - Z_b$ of 0.25 and 0.20 for the CuTi and Au_2Ta_3 structures are consistent with equal layer spacing as is a $Z_a + Z_b$ of $\frac{1}{2}$ for the former (see Fig. 1): a Z_b of $\frac{1}{3}$ indicates equal spacing in the $MoSi_2$ structure. The interplanar spacings are controlled by the relative sizes of the atoms and the relative strengths of bonding between layers, and, not surprisingly, the available crystallographic data for these structures indicate deviations from equal spacing. $Z_a - Z_b$ which are less than these values indicate that the spacing between an Au layer and an adjacent non-Au one is smaller than the average. Such contractions are consistent with the idea of strong bonding between unlike atomic species. In the $MoSi_2$ structure, a $Z_b > \frac{1}{3}$ corresponds to such a contraction (again see Fig. 1). This is calculated for $AuHf_2$, and, in general, crystallographic data for this structure indicates $0.33 < Z_b = 0.342$. We calculate a mild expansion for Au_2Hf. Here, the fact that Hf is a significantly larger atom than Au has caused the Au-Hf separation to be larger than the Au-Au and our value of Z_b, which is slightly less than $\frac{1}{3}$, seems more reasonable than the value of 0.34 which has been reported experimentally.

The $Z_a + Z_b$ plotted for AuHf in the γ-CuTi structure in Fig. 5 provides a measure of interplanar Au-Au versus Hf-Hf separation (as plotted in Fig. 1, Z_a measures the position of Hf planes and Z_b that of Au). The calculated $Z_a + Z_b$ of less than $\frac{1}{2}$ corresponds to Au-Au separation being smaller than those for Hf-Hf which is, again, consistent with Au being smaller than Hf.

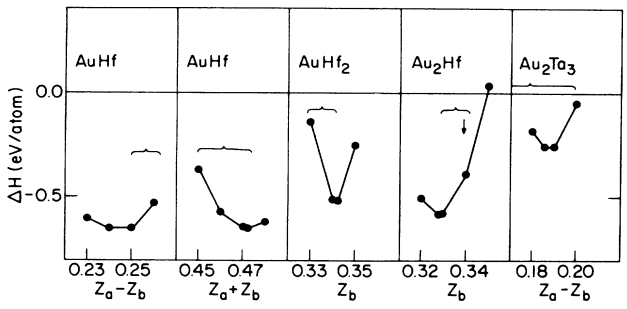

FIG. 5. Heats of formation of AuHf (γ-CuTi structure), $AuHf_2$, and Au_2Hf ($MoSi_2$ structure), and Au_2Ta_3 as a function of internal lattice coordinates (see Fig. 1 for their definition). The curly brackets indicate the ranges of values reported for these coordinates in other compounds of the same structure while the arrow, for Au_2Hf, is the value reported for this compound.

The most important aspect of the results of Fig. 5 is that the change in the ΔH with variations in these internal coordinates is substantial on the scale important to the accuracy required when comparing one phase with another as is done in Fig. 4. For example, the ΔH calculated for Au_2Hf at a Z_b of 0.34 would leave it slightly unbounded relative to a two-phase mix of AuHf and pure Au.

Returning to Fig. 4, consider now the Au-Pt system which is reported to be a disordered fcc phase except for Au_3Pt where it orders in the fcc Cu_3Au structure. We do not have results for disordered systems but we do see Au_3Pt to be stable relative to the lowest lying of the ordered 50%-50% phases, and we see that Pt_3Au, which is not observed, is calculated to be unstable relative to a two-phase mix of Pt and either AuPt or Au_3Pt. Note that we are dealing with small energy differences in this alloy system.

Finally, consider Au-Ta where Au_2Ta_3 is the most Au rich among the observed phases. The calculations are consistent with this, showing the suppression of the phases to its right. One of these is Au_2Ta, which is taken to be in the AlB_2 structure. This was chosen because Au_2Nb (and no other Au-transition-metal compound) is reported to have this structure. As already noted, the AlB_2 structure consists of graphitic planes of B's alternating with hexagonal Al layers of half the atomic density. The structure is thus ill packed with a smaller fraction of crystal volume accommodated in nonoverlapping atomic spheres than is the case for the other structures considered above. With the structure being ill packed, the muffin-tin potentials employed here should do worse when calculating its total energy. That its ΔH lies above the dashed line between Au_2Ta_3 and pure Au is to be expected, since the phase is not observed; however, there is the question of whether its ΔH should lie as far as it does above the line. Calculations for Au_3Ta and $AuTa_3$ in the Cu_3Au structure yield nonbinding ΔH's, which is consistent with the fact that they do not occur. The final result is for $AuTa_3$ in the ill-packed $A15$ structure which Au-Ta is reported to form in off-stoichiometry at a $AuTa_4$ composition. The ΔH for this phase should lie below the line between Ta and Au_2Ta_3 or perhaps, granted the question of stoichiometry, slightly above it. Instead it misses by about a 0.5 eV per atom. This provides a measure of the errors which can be introduced by employing muffin-tin potentials in calculations for systems of different packing and different local site symmetry.

V. CHARGE TRANSFER: COMPOUNDS IN THE CsCl STRUCTURE

As has been discussed previously,[5,6] the LASTO scheme provides a natural basis in terms of which population analyses can be done for valence charge in terms of s, p, and d orbitals centered on one site with their tails extending into others. The problem, of course, is the nonorthogonality between orbitals on different sites, and there is no completely satisfactory way of dealing with it. We have employed the Mulliken[9] and a modified

Mulliken[10] scheme for handling the nonorthogonality. One can instead sample the charge localized at a site by integrating the charge density over the Wigner-Seitz cell or sphere. We have integrated over the latter, which introduces small errors that we have corrected for by renormalizing the charge outside the muffin-tin spheres so that the correct total electron count is maintained.

The charge transfer on or off the Au sites, as measured with the three schemes, appears in Fig. 6 Here and throughout this paper by "charge transfer" we mean electron transfer; it is >0 for increased electron counts. The break at AuW in the molecular populations is symptomatic of the sensitivity of the results to the Slater-type-orbital basis sets and their orthogonalization. The three curves display similar shapes though with markedly different vertical positions. Starting with AuPt to the right, they rise as one moves to elements which are increasingly different from Au, *but* then they reverse and drop so that both the Mulliken and the WS sphere samplings indicate that Au loses charge to the very electropositive Lu. This is surprising. [The pairs of plotted points for AuLu and AuHf are associated with ambiguities in the definition of the WS spheres. These compounds suffer volume contractions, in the sense of Eq. (1), and one can apportion the contractions to both the Au and to Lu or Hf spheres equivalently or assign the contractions to the latter alone. The pairs of points represent the two choices.]

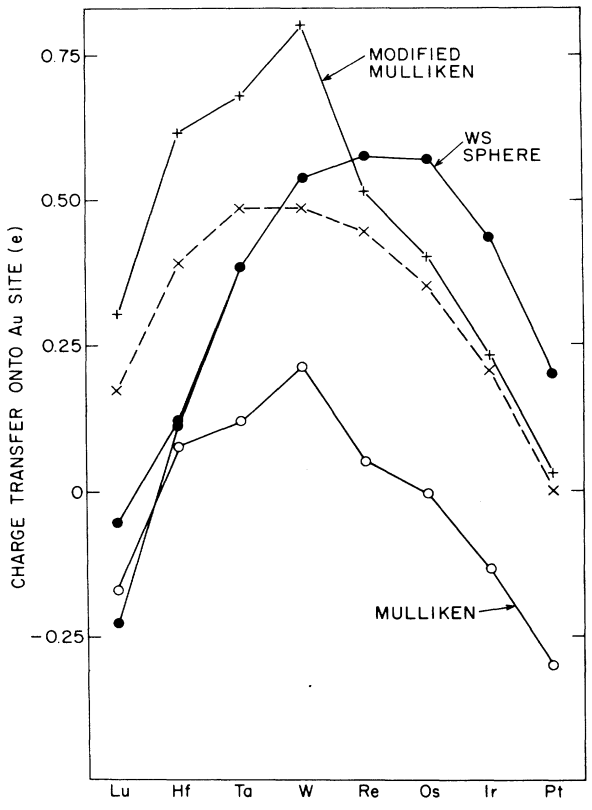

FIG. 6. Charge transfer on or off the Au site (positive for electron transfer to Au) for compounds in the CsCl structure as measured by WS sphere integrations and by Mulliken and modified Mulliken population analyses. The dashed curve involves an off-site attribution of the $l \geq 3$ WS sphere charge components as is discussed in text.

Certain features of Fig. 6 have an explanation which has nothing to do with the chemistry of *s*, *p*, or *d* electron transfer or screening. Consider Fig. 7; plotted is the total charge in orbital components, for $l \geq 3$, as calculated with LASTO and linear-augmented-plane-wave (LAPW) machinery for the elemental metals. These high-l components are a real feature of the charge density and they are best viewed (along with a bit of the *s*, *p*, and *d* components) as associated with the *tails of s-, p-, and d-band orbitals centered on other sites.* This charge is substantial, ranging from $\sim\frac{1}{20}$th of an electron for Lu to a $\frac{1}{4}$ for Os and Ir. Now, in the CsCl structure the eight nearest neighbors are unlike neighbors. What if these make a similar sampling of the tail charge in the compound? Different atoms with their different volumes will sample the tail charge differently. Let us assume that the sampling scales as the elemental volumes, i.e.,

$$\rho_B(l \geq 3) = \rho_A(l \geq 3)(V_B/V_A) , \tag{2}$$

where ρ_B is the *B*-site sampling in an *AB* compound and ρ_A is the elemental *A*-metal value from Fig. 7. Equation (2) is compared, in Fig. 8, with the charge associated with the $l \geq 3$ components obtained in the LASTO calculations for the compounds. The agreement for the Au and for the other sites is remarkable granted the assumptions implicit in Eq. (2).

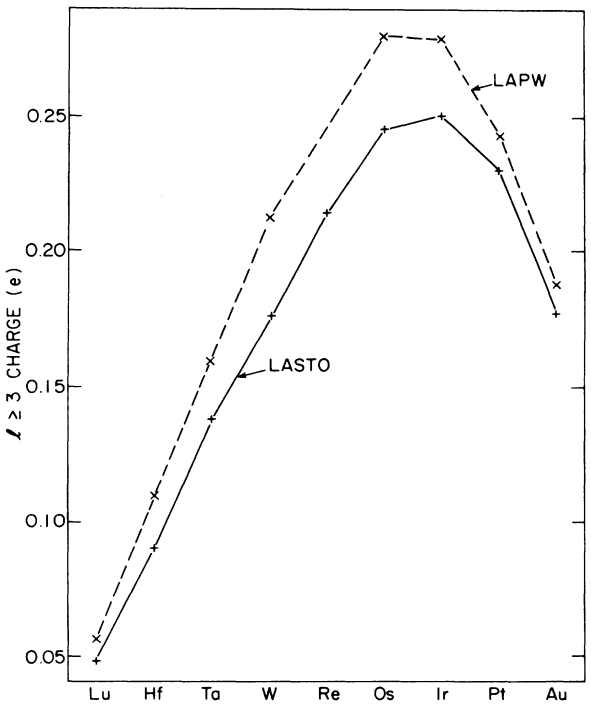

FIG. 7. The $l \geq 3$ charge components residing in the WS spheres of the elemental metals as obtained with LASTO and LAPW band calculations.

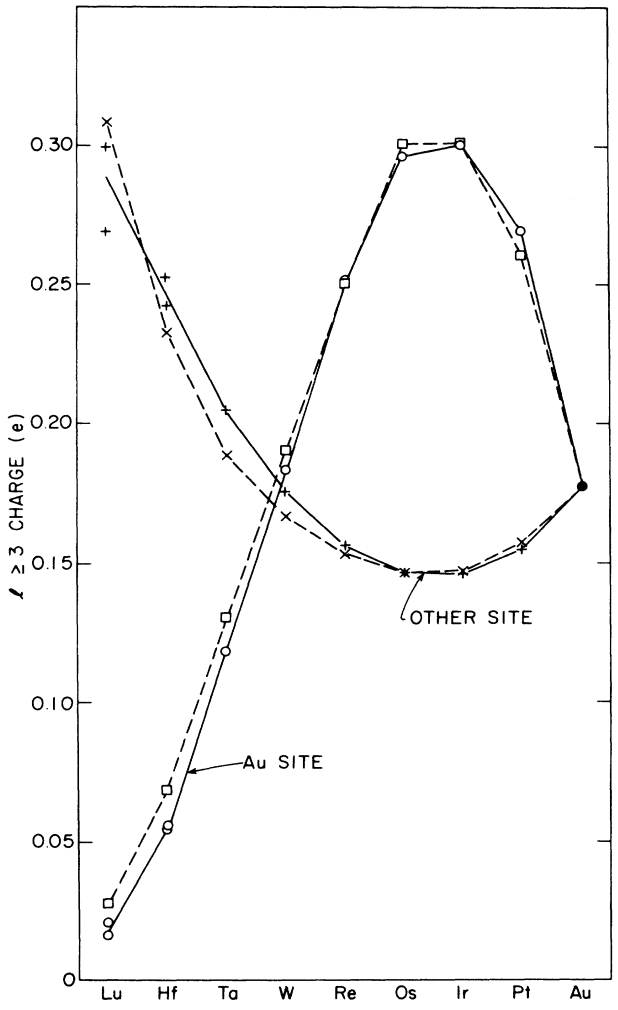

FIG. 8. The $l \geq 3$ charge components within the Au's and other element's WS spheres, as obtained with LASTO calculations for the CsCl structure compounds. The dashed curves are estimates based on scaling the elemental results of Fig. 7 with Eq. (2).

It would appear that a significant part of the "charge transfer" is due to such overlap effects. Taking the case of the CsCl structure compounds and attributing the $l \geq 3$ charge components to the eight closest neighbors, which are unlike, one can define

$$\rho_B \equiv \rho_B(l<3)+\rho_A(l \geq 3) \tag{3}$$

as the charge centered on a B site in these 50%-50% compounds. Doing this yields the dashed line curve of Fig. 6 which is in reasonable register with the two orbital population analyses, lying between them. This result also indicates that, in terms of charge centered on each site, charge transfer is always onto the gold.

The individual s, p, and d charge components are also of interest and plotted in Fig. 9 are the Mulliken and the WS sphere changes in d electron counts, Δn_d, at the Au and the non-Au sites. These are taken relative to the elemental metals. Though there are crossovers between AuHf and AuTa, the two samplings of the Δn_d's are similar. Au-site d charge is lost when alloyed with any of the $5d$ elements. This is to be expected: Elemental Au has filled d bands, but due to hybridization between bands there is about 9.5 electrons worth of d character in the 11 occupied conduction-electron states per atom. Hybridization of unoccupied wave-function character of the other alloy constituent into these states can only lower the Au-site d count. If that hybridization involved the other site's d-hole states (which they all have since their d bands are not filled), the Δn_d of the other site would be positive. This is the case for AuPt and AuIr, but not for the remaining alloys. It would appear that the Δn_d cannot be understood solely in terms of d-d hybridization. Also shown, to the right of the figure, are the changes in d count associated with going from fcc to bcc Au: These do not appear important to an understanding of the Δn_d associated with going from fcc Au to an Au compound in the bcc CsCl structure.

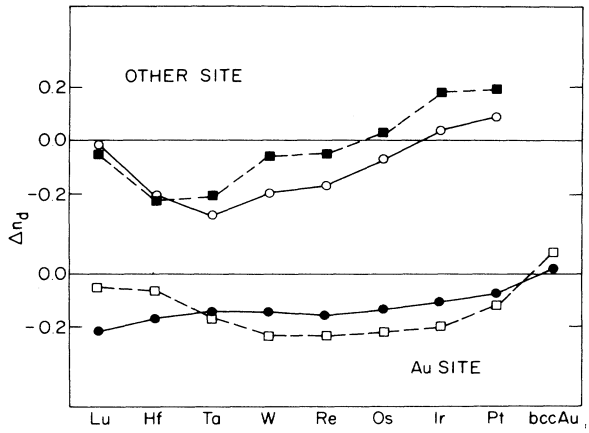

FIG. 9. Individual d charge transfer components at Au, and at the $5d$ sites alloyed with Au in the CsCl structure. Mulliken populations (dashed lines) and WS sphere integrations (solid lines) are shown. The charge count changes associated with taking Au from the fcc to the bcc structures are shown to the right.

The associated Δn_s and Δn_p appear in Fig. 10. Again, there is some tendency for the WS sphere and the Mulliken orbital population analyses to parallel one another though a break, in smooth character, is seen for the Au Mulliken Δn_p. This break was already seen in the total charge, Δn, counts in Fig. 6 and is associated with how details of the tails of the Slater-type orbitals affect the Mulliken treatment of the nonorthogonality. This is particularly important with the p orbitals which are more diffuse than their s and d counterparts. The break is symptomatic of the problems with such population analyses.

The Au site Δn_s, and for the most part the Δn_p, are opposite in sign to the Au Δn_d. This supports the view[2] that Au alloying involves d—non-d charge compensation where whatever the d electron transfer, the non-d transfer is the opposite. The same cannot be said for the other sites where as often as not, Δn_d has the same sign as $\Delta n_s + \Delta n_p$.

The most marked variation in a Δn_i is in the Au-site p term, and the most unusual feature which it shares with

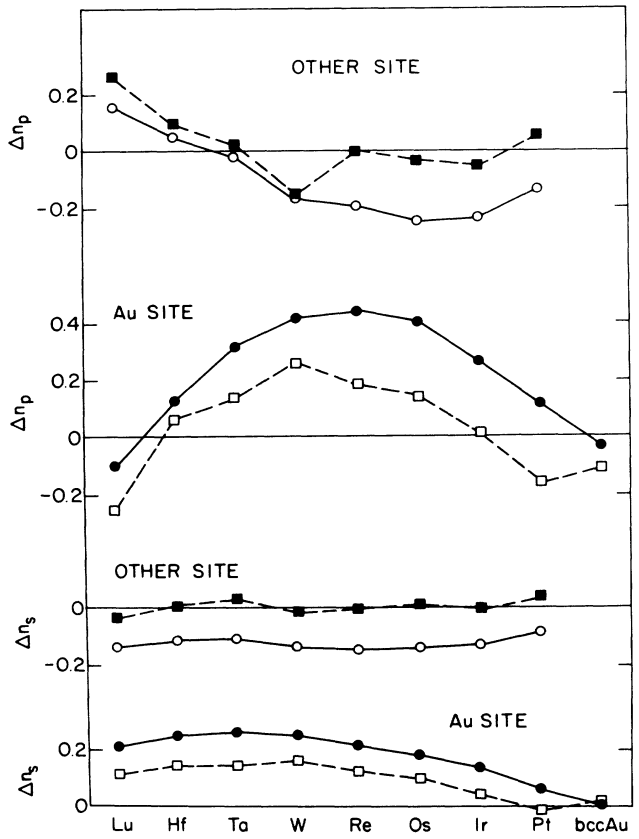

FIG. 10. Individual s and p charge transfer components at Au, and at the $5d$ sites alloyed with Au in the CsCl structure. Dashed lines indicate Mulliken population and the solid WS sphere samplings. The charge count changes associated with taking Au from the fcc to the bcc structure are shown to the right.

other Δn_i is that it does not vary monotonically as the $5d$ row is traversed but instead goes through an extremum.

A number of observables depend on charge transfer, one being the level shifts of core electrons as measured by photoemission. Both initial-state effects, associated with the chemical shift of the electron's one-electron energy, and final-state effects, associated with the changing screening of the hole left behind by the photoelectron, contribute to a measured level shift. Final-state effects often make substantial contributions[11] to the level shifts but will be neglected here. The initial-state excitation energy may be written as the electron's one-electron energy ϵ_i, measured with respect to the Fermi level ϵ_F. The level shift is then $\Delta(\epsilon_i-\epsilon_F)$, where $\epsilon_i-\epsilon_F$ of the compound of interest is measured with respect to some reference material such as the elemental metal. Calculated $\Delta(\epsilon_i-\epsilon_F)$ are plotted for the $4f_{5/2}$ core electrons in Fig. 11. Greater binding, that is negative $\Delta(\epsilon_i-\epsilon_F)$, would imply deeper potentials, hence charge transfer off a site. Except for PtAu and IrAu, there is increased binding at both sites; in fact, the $\Delta(\epsilon_i-\epsilon_F)$ correlate with the site Δn_d (see Fig. 9). This is not altogether surprising because the d charge is more compact than the valence s or p, causing it to have a

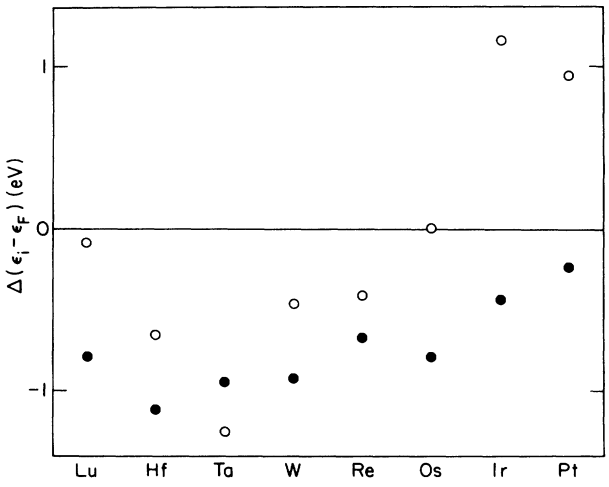

FIG. 11. The initial-state chemical shift $(\epsilon_i-\epsilon_F)$ for the $4f_{5/2}$ core level associated with going from the elemental metals to the compounds in the CsCl structure.

substantially larger Coulomb interaction[2] with a core electron. It would appear that the initial-state contribution to the core-level shift—any comparison with experiment must also consider final-state screening—is dominated by the effects of changing d electron count on the local potential.

Mössbauer isomer shifts provide a very different measure of the valence charge density, since they sample changes in the charge density at the nucleus which is associated with s (and relativistic $p_{1/2}$) electrons. A survey[3] of isomer-shift data for transition elements, as impurities in other transition-metal hosts, suggested that the isomer shifts arose from changes in valence s electron count *and* also from the screening of the valence-electron charge, already present, due to changing non-s count. Data for different impurities suggested that the balance of these contributions varies as a transition-metal row is traversed. Recently, Akai *et al.* have done calculations[12] for the isomer shift at a host Fe site immediately adjacent to a substitutional impurity. In this case the isomer shift can be understood in terms of the change in s-electron count alone. It is of interest to see what the behavior is for the 50%-50% alloys considered here. The quantity

$$\frac{\Delta\rho(0)}{\rho(0)}\equiv\frac{\rho_c(0)-\rho(0)}{\rho(0)} \tag{4}$$

is plotted in Fig. 12(a), where $\rho(0)$ is the calculated valence-electron density at the nucleus in the elemental metal and $\rho_c(0)$ is the density at that element's nucleus in the compound. (This quantity might be better normalized by multiplying by $\frac{4}{3}$, since the elemental metals all have $\sim\frac{3}{4}$ of an s electron's charge in the WS sphere.) The Au site contact density increases monatonically as Au is alloyed with elements further and further from Au while the other sites display a loss in contact density. This is consistent with the signs of the WS sphere samplings of Δn_s, and Fig. 12(b) is obtained by dividing $\Delta\rho(0)/\rho(0)$ by Δn_s. This provides an indication of the change in contact density per change in s-electron count (the local s count as

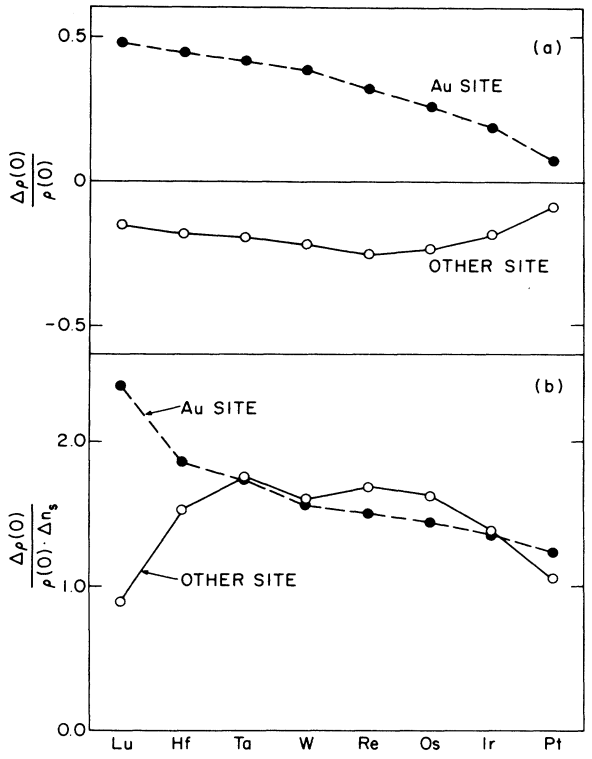

FIG. 12. Normalized changes in the conduction-electron contributions to the contact density at the nucleus associated with going from the elemental metals to the compounds in the CsCl structure. (a) $\Delta\rho(0)/\rho(0)$ and (b) $\Delta\rho(0)/\Delta n_s\rho(0)$; see text.

measured within the WS sphere is appropriate for this purpose). The $\Delta\rho(0)$, so normalized, again rise monotonically for Au while showing a dropoff, at the other site, for Lu and Hf. For the most part, the values are well above 1 in magnitude, so that the $\Delta\rho(0)$ cannot be due to the simple addition or subtraction of s charge if that s charge is to have a contact density resembling that appropriate to the average s density in the elemental metal. More important than the magnitude of any particular $\Delta\rho(0)/\rho(0)\Delta n_s$ is the variation in this quantity which is not readily understood unless screening of the s charge by other charge transfer terms is involved. It would appear that these alloys display behavior similar to that of the dilute alloys and not that of an iron host's response to impurities.

VI. CHARGE TRANSFER WITH VARYING COMPOSITION

Charge transfer is expected to change with varying composition and with differing structure at some given composition. This is seen to be the case for the Au-Hf and Au-Ta systems in Fig. 13, where the sum $\Delta n_s+\Delta n_p+\Delta n_d$ is plotted as a function of Au concentration. The majority atom's sum should, on average, go to zero as its weight approaches one, and the dashed lines drawn to guide the eye have such zero intercepts. It might be expected that the sum for the minority atom

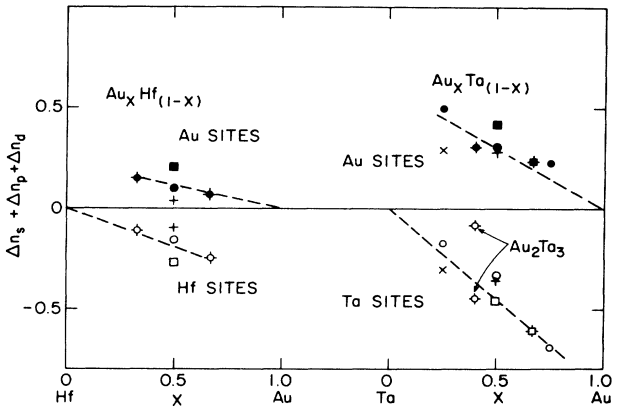

FIG. 13. Charge transfer, taken as $\Delta n_s+\Delta n_p+\Delta n_d$, in the Au-Hf and Au-Ta systems as a function of composition. See Fig. 4 for the structures associated with different symbols; here the solid symbols indicate Au results and the open symbols represent Hf and Ta.

would saturate as its weight goes to zero. There is no indication of saturation in the present results but this may merely reflect that sufficiently dilute compounds were not dealt with.

There is a significant spread in the sum for different structures with CsCl the most "ionic" of the 50%-50% compounds. The eight atoms in this structure's nearest-neighbor shell are all unlike atoms, while $\frac{2}{3}$ of the 12 nearest neighbors are unlike neighbors in the CuAuI structure and only $\frac{1}{3}$ are in the γ-CuTi structure. The charge transfer in AuHf follows this sequence, while the AuTa the latter two structures have essentially identical sums. The situation is more complicated for Ta_3Au, for which there are results for the $A15$ and Cu_3Au structures. Here the former is the more "ionic" at the minority site and less so at the majority. This, like the fact that the Au sites appear to sustain less transfer than do Hf and Ta (note the slopes of the dashed lines), is associated with the fourth component of the charge transfer, namely the tail charge as manifested in the $l\geq 3$ components of the density. Remember that the Au tails transfer more charge into the Ta and Hf sites than their tails do back onto the Au.

There are two points in Fig. 13, associated with the two Ta sites in Ta_3Au_2 (See Fig. 1). The site with no nearest Au neighbors has the near-zero transfer, while there is substantial transfer at the sites with the Au neighbors. All individual Δn_i terms are small at the isolated site, and its contact density at the nucleus is close to that of bcc Ta. There is a 0.7-eV difference in the $4f$ core-electron one-electron energies between the two Ta sites with the isolated one, with its greater site charge, being the less bound.

VII. DISCUSSION

There have been relatively few studies of the heats of formation of intermetallic compounds in the $5d$ row, and there are apparently no experimental data for the Au compounds among these. Williams, Gelatt, and Moruzzi[13] have carried out calculations for a large number of al-

loys in the $4d$ row and have used their results to argue in favor of the d bond model put forward by Pettifor[14] and extended by Watson and Bennett.[15] Recently, Robbins and Falicov[16] have further extended the d bond model to include s and p bands and the effects of disorder. Disorder has also been treated within a tight-binding coherent-potential approach by Gautier and co-workers.[17] Our calculations are most similar to those of Williams *et al.* based directly on density-functional theory and treating ordered compounds. Theirs differ from ours in the method of solving the density-functional equations; they use the augmented-spherical-wave method[18] with overlapping spheres while we use the augmented-Slater-type-orbital method with a muffin-tin potential (no overlapping spheres). Cohesive and structural energies for the elements have been reported elsewhere.[6] In addition, we have calculated[10] the heats of formation of TaIr and HfPt for which experiments do exist and found good agreement with experiment. We have also calculated the heat for Cu_3Au (Ref. 19) for which we obtain -0.05 eV/atom in good agreement with experiment which is -0.04 eV/atom. There is certainly the possibility of a muffin-tin error in these heats. It is important to calculate the energy of the elemental metals with the same muffin-tin radius as used in the compound (which is generally smaller than the touching sphere value for the elemental metal). As indicated by our results for the $A15$ compound, the muffin-tin approximation is apparently breaking down for ill-packed structures, which is consistent with other calculations on $A15$'s.[20] However, for the close-packed structures our results are all consistent with known phase-diagram behavior.

The dominant trend in the heat of formation has been elucidated by Pettifor.[14] He adopts a tight-binding description of the d bands and neglects the s and p altogether. In the elements, as shown by Friedel,[21] if one further assumes a rectangular density of states then the heat of formation is simply

$$\Delta = -n(10-n)w/10 , \tag{5}$$

where n is the d electron number (10 for gold, 9 for Pt, etc.) and w is the bandwidth. For the AB alloy with $n_B > n_A$ Pettifor uses a moment argument to find

$$w_{AB} = (w^2 + 3\delta^2)^{1/2} , \tag{6}$$

where $\delta = e_A - e_B$ is the difference in the band centers of the A and B constituents. He assumes $\delta = k(n_B - n_A)$, k being a constant, and the heat of formation becomes

$$\Delta_{AB} = -\frac{\bar{n}(10-\bar{n})}{20}(w_{AB} - w) + \tfrac{1}{4}k\,\overline{\Delta n} , \tag{7}$$

were $\bar{n} = (n_A + n_B)/2$ and $\Delta n = n_B - n_A$. Pettifor has chosen $k = 1$ eV and $w = 10$ eV and with these values obtains heats in very rough agreement with our calculations. Certainly the trend displayed in Fig. 2 is reproduced, although this formula gives no binding (i.e., a positive heat) for AuPt and underestimates the binding for AuLu and AuHf by ~ 0.25 eV. Since the trend is correct, we can ask why it occurs. According to Eq. (7) binding comes about from a balance of three terms. The first is the attraction which comes from lowering the Fermi level of the B electrons, the second the attraction due to the larger bandwidth in the alloy, and the third the repulsion due to raising the B electrons from e_B to an average energy $(e_A - e_B)/2$. The A electrons are, of course, lowered from e_A to the average energy, but $n_B > n_A$, so this term always costs energy. The bandwidth term produces maximum binding for $\bar{n} = 5$ (for fixed Δn) and goes to zero for $\bar{n} = 0$ or 10. Therefore, alloys tend to form for $\bar{n}$ near 5 and not form at the end points. AuPt with $\bar{n} = 9.5$ is therefore suppressed, but as $\bar{n}$ decreases the bandwidth term gradually wins out and so the Ta, Hf, and Lu alloys form. Our calculations are consistent with this result, although with such a delicate interplay of conflicting energies it is amazing that the simple model works out so well.

In contrast, the d bond model fails when it comes to charge transfer. This is because the charge flow involves s and p electrons to a very great extent. Indeed, for many of the alloys both constituents lose d electrons which cannot be explained in a d only model. These s and p rearrangements, though large, must not have an important effect on the energetics. Consistent with this, the model calculations of Robbins and Falicov[6] indicate that the effect of turning off s-d hybridization is to change the heats by ~ 0.01 ev.

More generally, the concept of electronegativity does not apply to these charge transfers. Any electronegativity scale would give a larger electron transfer to the gold as the other element moves to the left in the Periodic Table. This is not the case. As was already noted, the total charge transfer onto Au (Fig. 6) increases on going from Au alloyed with Pt to when it is alloyed with W, but then there is a reversal with the electropositive element Hf, and in turn Lu, involved in markedly less transfer. Inspection of the individual s, p, and d components, plotted in Figs. 9 and 10, for the non-Au sites show this reversal to be associated with p and d charge components which started negative and are going to zero in the case of Δn_d and reversing sign in Δn_p. Now the d bands of elemental Lu and Hf are largely empty and there is a significant amount of p character hybridized in both the occupied and unoccupied bands in the vicinity of the Fermi level. As the bands are emptied, on going from W to Lu there are fewer occupied levels into which Au character can be hybridized (hence reducing the loss of charge at these other sites) and there are more empty levels which can be hybridized into the occupied Au bands (also reducing the charge loss). It would appear that the emptying of the d bands and the associated lack of appropriate states to sustain the charge depletion leads to the reduction in charge transfer for Hf and Lu. The associated loss of gained charge on the Au site is, of necessity, s-p in character and from Fig. 10 it would appear to be primarily p-like.

We note that d-electron charge transfers opposite to electronegativity[22] can occur in the "covalent limit" where the bandwidth is much larger than the separation in average energy of the constituents. In that case, both sites tend towards equal electron counts in the alloy given by n_d, which implies a gain of electrons by the A element and a loss by B. This would be expected to be most likely for elements near each other in the Periodic Table rather

than for those separated by a large amount, and this is obtained for the d charges of AuPt and AuIr.

VIII. CONCLUSION

The alloying of Au with its $5d$-transition-element neighbors, Lu through Pt, has been considered. Total energies were calculated using muffin-tin local-density potentials. While there are no experimental heats of formation for these compounds, the calculated heats appear to be reasonable and in accord with the known phase-diagram behavior. Calculations were done for a number of alloy compositions and for a variety of crystal structures, most of which were close-packed (bcc-, fcc-, and hcp-like) systems. Overall, the calculations successfully predicted the stable phase at some given composition and the relative stabilities of phases at differing compositions. The notable exception occurred for $AuTa_3$ in the $A15$ structure which is significantly worse packed than the other systems: This is a stable phase (actually off 3:1 stoichiometry) in the Au-Ta system and the calculated heat of formation was off by a substantial margin. This could be due to either shortcomings in the LASTO basis or to the use of muffin-tin potentials. Preliminary LAPW calculations, also employing muffin-tin potentials (and with limited sets of k points) yield a heat of formation for this compound which is in agreement with the LASTO result. This would suggest that the problem lies with the muffin-tin potentials. Earlier band-theory investigations[20] of the band structures and charge densities of $A15$ compounds (total energies were not calculated) came to the same conclusion.

Charge transfer was also considered. In the case of the Au sites, the initial-state core-level shifts indicate valence charge transfer off, while the contact densities at the nucleus indicate transfer onto Au. This was observed experimentally some years ago and recognized[2] as evidence of d transfer off and non-d onto Au during alloying. This is consistent with the individual shell Δn_i as obtained with either the orbital population analyses or by integration over the WS spheres. The situation is different at the sites of the atoms alloyed with Au where, as often as not, the d transfer is in the same direction as the non-d. The Δn_i as obtained in the population analyses and in the WS spheres show many features in common, although they are sufficiently out of register to make definitive quantitative statements concerning such transfer impossible. Nevertheless, the resulting charge transfer is inconsistent with simple electronegativity arguments *and* with models which assume only d-band hybridization.

There is one feature of the charge transfer which is trivially obvious but which to our knowledge has not been discussed previously in the literature. It concerns the high-l components of the charge density at any site which are associated with the tails of wave functions centered on other sites. The nonorthogonality associated with this tailing complicates the orbital population analyses and is the principle source of disparities between such results and the WS sphere samplings. Because the amount of such tailing charge varies from element to element, there is a charge transfer contribution at a site which depends on what atoms are neighbors to the site. This "overlap" charge transfer, which has nothing to do with chemical band hybridization or charge screening effects, is a significant source of the charge transfer occurring in the alloys considered here.

ACKNOWLEDGMENT

Work supported by Division of Materials Sciences, U.S. Department of Energy under Contract No. DE-AC02-76CH00016 and by an allocation of computer time at the National Magnetic Fusion Energy Computer Center at Lawrence Livermore Laboratory.

[1]For example, W. Hume-Rothery, in *Phase Stability in Metals and Alloys*, edited by P. S. Rudman, J. Stringer, and R. I. Jaffee (McGraw-Hill, New York, 1967), p. 3; for a recent theoretical accounting, see G. M. Stocks, M. Boring, D. M. Nicholson, F. J. Pinski, D. D. Johnson, J. S. Faulkner, and B. L. Gyorffy, in *Noble Metal Alloys*, edited by T. B. Massalski, W. B. Pearson, L. H. Bennett, and Y. A. Chang (TMS-AIME, Warrendale, PA, 1985), p. 27.

[2]R. E. Watson, J. Hudis, and M. L. Perlman, Phys. Rev. B **4**, 4139 (1971); R. M. Friedman, J. Hudis, M. L. Perlman, and R. E. Watson, *ibid.* **8**, 2433 (1973); T. S. Chou, M. L. Perlman, and R. E. Watson, *ibid.* **14**, 3248 (1976); T. K. Sham, R. E. Watson, and M. L. Perlman, in *Mössbauer Spectroscopy and Its Chemical Applications*, edited by J. G. Stevens and G. K. Shenoy (American Chemical Society, Washington, D.C., 1981).

[3]For example, R. E. Watson, L. J. Swartzendruber, and L. H. Bennett, Phys. Rev. B **24**, 6211 (1981).

[4]For example, R. E. Watson and L. H. Bennett, Acta Metall. **30**, 1941 (1982).

[5]J. W. Davenport, Phys. Rev. B **29**, 2896 (1984).

[6]J. W. Davenport, M. Weinert, and R. E. Watson, Phys. Rev. B **32**, 4876 (1985); J. W. Davenport, R. E. Watson, and M. Weinert, *ibid.* **32**, 4883 (1985).

[7]See, in particular, P. Villars and L. D. Calvert, *Pearson's Handbook of Crystallographic Data for Intermetallic Phases* (American Society for Metals, Metals Park, Ohio, 1985); for Au_2Ta_3, see E. Raub, and D. Menzel, Z. Metallk. **52**, 831 (1961).

[8]For example, see L. Ansara, Int. Metall. Rev. **24**, 20 (1979); J. W. Cahn, Bull. Alloy Phase Diag. **1**, 27 (1980).

[9]R. S. Mulliken, J. Chem. Phys. **23**, 1833 (1955).

[10]R. E. Watson, J. W. Davenport, and M. Weinert, Phys. Rev. B **34**, 8421 (1986).

[11]M. Weinert, J. W. Davenport, and R. E. Watson, Phys. Rev. B **34**, 2971 (1986).

[12]H. Akai, S. Blügel, R. Zeller, and P. H. Dederichs, Phys. Rev. Lett. **56**, 2407 (1986).

[13]A. R. Williams, C. D. Gelatt, Jr., and V. L. Moruzzi, Phys. Rev. Lett. **44**, 429 (1980).

[14]D. G. Pettifor, Phys. Rev. Lett. **42**, 846 (1979); Solid State Commun. **28**, 621 (1978).

[15]R. E. Watson and L. H. Bennett, Phys. Rev. Lett. **43**, 1130 (1979); CALPHAD: Comput. Coupling Phase Diagrams Thermochem. **8**, 307 (1984).

[16]M. O. Robbins and L. M. Falicov, Phys. Rev. B **29**, 1333

(1984).
[17]See, e.g., A. Bieber and F. Gautier, Solid State Commun. **38**, 1219 (1981).
[18]A. R. Williams, J. Kübler, and C. D. Gelatt, Jr., Phys. Rev. B **19**, 6094 (1979).
[19]J. W. Davenport, R. E. Watson, and M. Weinert (unpublished).
[20]L. F. Mattheiss and D. R. Hamann, Solid State Commun. **38**, 689 (1981), and references therein.
[21]J. Friedel, *The Physics of Metals,* edited by J. M. Ziman (Cambridge University Press, Cambridge, England, 1969), Chap. 8.
[22]R. E. Watson and L. H. Bennett, Phys. Rev. B **18**, 6439 (1978).